ELSEVIER

Marine Geology 161 (1999) 1–12

MARINE GEOLOGY
INTERNATIONAL JOURNAL OF MARINE GEOLOGY, GEOCHEMISTRY AND GEOPHYSICS

www.elsevier.nl/locate/margeo

The structure and segmentation of the Southeast Indian Ridge

Christopher Small [a,*], James R. Cochran [a], Jean-Christophe Sempéré [b,1], David Christie [c]

[a] *Lamont-Doherty Earth Observatory, Palisades, NY 10964, USA*
[b] *School of Oceanography, University of Washington, Seattle, WA 98195, USA*
[c] *College of Oceanography, Oregon State University, Corvallis, OR 97331, USA*

Received 20 May 1996; accepted 18 September 1998

Abstract

The Southeast Indian Ridge (SEIR) spreads at a relatively narrow range of intermediate rates (59–75 km/Ma) but exhibits the full range of slow to fast spreading morphology and segmentation. Satellite gravity data reveal transitions in the structure of the spreading center where it is influenced by the Amsterdam and Kerguelen hotspots and at the Australian–Antarctic Discordance (AAD). Although the spreading rate between the hotspots and the AAD is nearly constant, the ridge exhibits a variety of distinct styles of morphology and segmentation not observed at fast or slow spreading centers. Recently, collected multibeam bathymetry data reveal a transition from East Pacific Rise style overlapping axial highs near 92°E to Mid-Atlantic Ridge style axial valleys with non-transform offsets near 116°E. The intervening segmentation is characterized by propagating offsets coexisting with stationary transforms which exhibit different degrees of temporal stability. Currently, there are 10 transform offsets between the hotspots and the AAD but only five of these have persisted since seafloor spreading stabilized at 35 Ma. The other five appear to have formed since 35 Ma and several more have disappeared by transform shortening or coalesced by along-axis propagation. There is a transition from monotonic offset propagation near the hotspots to oscillatory propagation approaching the AAD. This change in offset stability corresponds to transitions in depth, axial morphology and offset structure. Through much of the transitional region, higher order segmentation is characterized by en-echelon offsets of a diffuse spreading axis that generally lacks a well defined neovolcanic zone. Since the spreading rate is nearly constant, the regional variation in axial morphology and segmentation appears to be controlled by an upper mantle thermal gradient — possibly a result of flux of asthenosphere from the hotspots to the AAD. This is consistent with the gradual increase in average ridge flank depths along this part of the plate boundary but segment scale changes in axial depth reveal spatio-temporal variability in the dynamic topography that are not preserved on older lithosphere. Intrasegment transitions in axial morphology and en-echelon offsets within first order segments suggest that local variations in mantle thermal structure introduce short-lived instabilities in higher order segmentation and dominate the short term evolution of the plate boundary.

Keywords: Southeast Indian Ridge; structure; segmentation

1. Introduction

Much of our knowledge of mid-ocean ridge dynamics is based on studies of the fast and slow

* Corresponding author. Tel.: +1-914-3658354; E-mail: small@1deo.columbia.edu

[1] Now at Exxon Production Research, P.O. 2189, Houston, TX 77252, USA.

0025-3227/99/$ - see front matter
PII: S0025-3227(99)00051-1

spreading endmembers of the system, primarily the northern Mid-Atlantic Ridge and the northern East Pacific Rise. In order to understand the fundamental processes of lithospheric accretion at mid-ocean ridges it is necessary to determine what controls the differences in morphology and segmentation observed at different spreading rates. The Southeast Indian Ridge (SEIR) spreads at a relatively narrow range of intermediate rates (59–75 km/Ma) but appears to be influenced by both anomalously hot and cold upper mantle structures. As a result, it contains morphology and segmentation styles spanning the entire range observed at mid-ocean ridge plate boundaries and provides an opportunity to investigate the factors that control the transition between the end members. Mid-ocean ridges are often parameterized by spreading rate because it kinematically exerts a first order control on both the deformation rate and thermal structure of the plate boundary. The thermal structure, in turn, controls both the mechanical strength of the lithosphere and the dynamics of melting and upwelling in the advected asthenosphere. The SEIR is a particularly important place to study mid-ocean ridge processes since the kinematically driven advection and deformation rates are fixed by the constant spreading rate while the plate boundary is subject to both local and regional thermal perturbations.

During the austral summer of 1994–1995 an extensive geophysical/geochemical exploration of the SEIR was conducted aboard the R/V *Melville*. Over 188,000 km^2 of seafloor were mapped along the ridge from 88°E to 119°E. Multibeam bathymetry and sidescan sonar, free air gravity, and magnetic anomaly data were collected and rock samples were recovered from 104 dredges and wax cores. With this multidisciplinary program, one of the least explored sections of the global mid-ocean ridge system has now become one of the most thoroughly surveyed and sampled. Overviews of the gravity and morphology of the SEIR are given by Cochran et al. (1997) and Sempéré et al. (1997).

The complexities of the kinematic evolution of the Indian Ocean basin have been reconstructed in great detail in a series of seminal works (e.g., Schlich and Patriat, 1967; LePichon and Heirtzler, 1968; McKenzie and Sclater, 1971; Sclater and Fischer, 1974; Schlich, 1975, 1982; Royer and Schlich, 1988) but the dynamical evolution of the SEIR itself is still not well understood. The purpose of this study is to summarize the regional systematics in the structure and segmentation of the SEIR both at present and over the past ~35 Ma. The evolution of the large scale segmentation is interpreted from satellite gravity data (Sandwell and Smith, 1997) while present-day segmentation of the transitional region between 88°E and 117°E is investigated using recently collected multibeam bathymetry data. Detailed discussions of the recently collected multibeam sonar, gravity and magnetic anomaly data as well as rock samples from the ridge axis are given in a series of related studies (e.g., Christie et al., 1995; Cochran et al., 1997; Goff et al., 1997; Sempéré et al., 1997; Ma and Cochran, 1997; Shah and Sempéré, 1998).

2. Regional segmentation and structure of the SEIR

The structure and segmentation of the SEIR are dominated by the presence of three external influences on the mantle thermal structure. The Amsterdam and the Kerguelen hotspots, near 70°E–80°E, are a source of elevated mantle temperatures (Roult et al., 1994) while the Australian–Antarctic Discordance (AAD), near 120°E–125°E, is believed to be the location of anomalously low mantle temperatures (Vogt et al., 1984; Forsyth et al., 1987). The planform segmentation and morphology of the SEIR changes significantly in the vicinity of the on-axis Amsterdam St. Paul hotspot (ASP) and apparently continues to be influenced by the Kerguelen hotspot which now lies ~1000 km to the southwest of the spreading center. The region around the on-axis Amsterdam hotspot marks a transition between typical slow spreading morphology and transitional intermediate morphologies (Royer, 1986; Small et al., 1989). To the northwest of Amsterdam the plate boundary is characterized by numerous short (100–200 km) first order segments and well developed axial valley morphology (Royer and Schlich, 1988; Ma and Cochran, 1996). To the southeast of Amsterdam the plate boundary is characterized by longer (200–500 km) first order segments and more subdued axial

ridge morphology (Ma and Cochran, 1996). The segmentation and morphology change even more abruptly at the AAD as extensively segmented axial valleys abut longer westward propagating axial ridges across a single transform at the eastern boundary (Weissel and Hayes, 1974; Palmer et al., 1993; Christie et al., 1995). The section of the ridge axis between Amsterdam and the AAD exhibits a more gradual transition from fast spreading morphology and segmentation near the hotspots and slow spreading morphology and segmentation near the AAD.

Present-day variations in segmentation style and morphology along this part of the plate boundary are believed to reflect regional and local variations in mantle temperature because the spreading rate changes relatively little between the Amsterdam hotspot (65 km/Ma) and the AAD (76 km/Ma). Variations in axial depth and subsidence rate along the SEIR suggest persistent fundamental differences in the process of lithospheric accretion along axis (Cochran, 1986; Hayes and Kane, 1994) and a gradient in mantle structure is suggested by seismic tomographic models (e.g., Roult et al., 1994; Su et al., 1994). This range of intermediate spreading rates produces metastable axial morphology which is more sensitive to local thermal perturbations than the stable morphologies at higher and lower spreading rates (Small and Sandwell, 1989; Chen and Morgan, 1990a,b; Small, 1995). The transitional axial morphology in this area is discussed in detail by Cochran et al. (1997), Sempéré et al. (1997) and Shah and Sempéré (1998).

The segmentation of the plate boundary and its temporal evolution also highlights the importance of thermal perturbations. The recent (20 Ma) evolution of the segmentation of the spreading center west of 84°E is discussed in detail by Royer and Schlich (1988) who confirmed an absolute northeastward migration of the western SEIR by preferential accretion onto the Antarctic plate as predicted by the asymmetric spreading model of Stein et al. (1977). The most prominent feature in the regional planform segmentation of the SEIR is a southwestward displacement of the plate boundary east of the Amsterdam massif. Royer and Schlich (1988) show a change in the sense of asymmetric spreading in which the Indian plate has accreted faster on the two segments immediately to the southeast of the massif. This suggests that the thermal influence of the Kerguelen hotspot has retarded the northeastward migration of these two segments relative to the rest of the plate boundary during the past 40 Ma (Small, 1995). The other prominent feature in the regional segmentation of the spreading center is the AAD more than 2500 km to the east where a series of short stable segments have persisted almost since the initiation of seafloor spreading (e.g., Vogt et al., 1984; Marks et al., 1991; Palmer et al., 1993).

3. Evolution of segmentation on the SEIR since 40 Ma

The kinematic spreading history of much of the SEIR has been determined but a detailed understanding of the segmentation of the SEIR has been hampered by a paucity of magnetic anomaly profiles for the areas east of 79°E. Evolution of the SEIR prior to 35 Ma is poorly constrained because of the complexity of the formation and rifting of Broken Ridge that resulted from interaction between the Kerguelen hotspot and the migrating spreading center. The recent availability of satellite gravity data (Sandwell and Smith, 1997) for this entire region provides costraints on the evolution and temporal stability of the first order segmentation. These data offer moderate resolution ($\lambda > 35$ km; Small and Sandwell, 1994) coverage of the marine free air gravity anomalies and in many cases can discriminate even narrower features if they are spatially contiguous. The regional gravity map in Fig. 1 clearly shows the fracture zones marking the first order segmentation of the SEIR since spreading stabilized shortly after the rifting of Broken Ridge.

These gravity data indicate that the plate boundary between the Rodriguez triple junction and the George V fracture zone has been characterized by 17 stable first order segments since its reorientation after crossing the Kerguelen hotspot at $\sim$40 Ma. These 17 segments (indicated by roman numerals) are referred to here as zero order segments to distinguish them from those first order segments (as defined by Macdonald and Fox, 1988) that have persisted for more than 4 Ma but not necessarily since

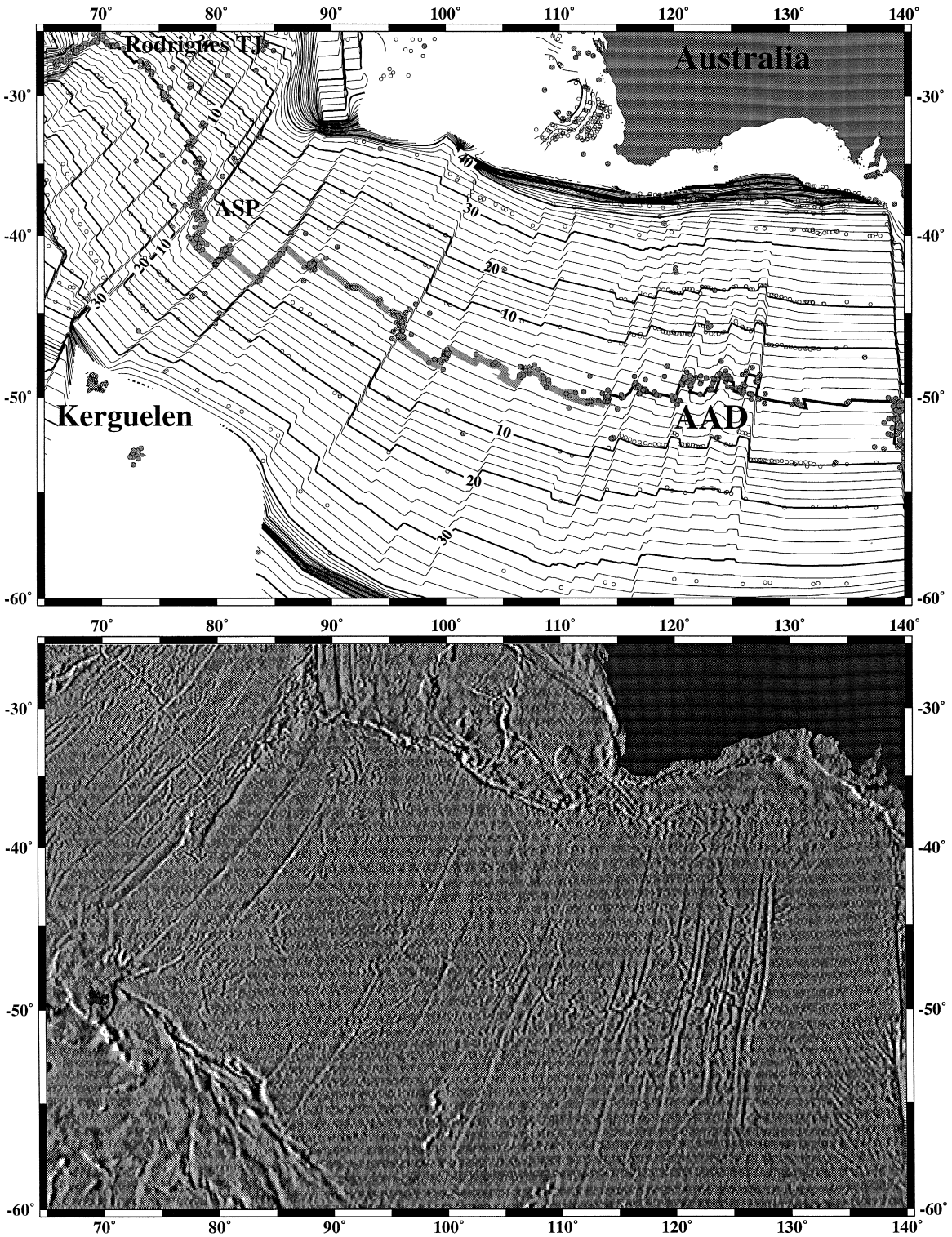
70˚
80˚
90˚
100˚
110˚
120˚
130˚
140˚
-30˚
-40˚
-50˚
-60˚
Rodrigues TJ
Australia
ASP
AAD
Kerguelen
10
20
30
40

the onset of stable spreading. At present, the plate boundary between 88°E and 116°E is composed of eight first order segments (Fig. 2), four of which are zero order segments. In the past it may have been composed of as many as 11 first order segments bounded by stable transforms now preserved as fracture zones on the ridge flanks. In an earlier study, based on underway data, Hayes and Kane (1994) identified five stable spreading segments on the SEIR. The boundaries of these segments coincide with those of five of the 17 zero order segments described here. The other boundaries were not clearly identifiable in the underway dataset because of its sparse coverage. The importance of the stable segmentation, recognized by Hayes and Kane (1994), can now be considered in the context of migrating offsets.

The zero order segmentation of the SEIR is remarkable in that it has persisted in the presence of numerous migrating offsets. Furthermore, there appears to be little correlation between the persistence of the zero and first order segments and either segment length or offset distance. For example, segment III is over 700 km long while the adjacent segment IV is less than 70 km long. The satellite gravity map in Fig. 1 indicates that at least two eastward propagating offsets have traversed the length of segment III terminating at the boundary of segment IV while segment IV has persisted intact for the duration of the current episode of seafloor spreading. Segment IV seems to have shifted at $\sim$ 20 Ma but remained intact. At present, the offsets bounding segment IV are $\sim$ 90 km long on the west and less than 40 km long on the east. Without complete flowline parallel magnetic anomaly data it is not possible to constrain the length of the offsets in the past but the persistence of a fracture zone anomaly in the satellite gravity data verifies the temporal stability of these boundaries. In contrast, many other first order segments are transient and may appear and disappear by lenthening and shortening of the transform offset.

The first order segmentation also appears to have undergone a major transformation around 18 Ma when the spreading rate decreased (e.g., segment IV, Fig. 1). This is evident in the appearance of several fracture zones, particularly within the AAD, during this time. The decrease in spreading rate appears to have prompted a number of previously stable segments to subdivide into shorter segments bounded by transform offsets producing fracture zones that are still prominent on the ridge flanks.

The satellite gravity data shown in Figs. 1 and 2 indicate that the transform at 100°E marks a boundary in both past and present-day segmentation and structure of the SEIR. West of 100°E the segmentation is generally characterized by unidirectional, monotonic eastward propagation of offsets. East of 100°E the segmentation is dominated by oscillatory offset propagation since the initiation of seafloor spreading between Australia and Antarctca (e.g., 40°S 122°E and 53°S–58°S 97°E–98°E). The oscillatory propagation described here is analogous to duelling propagation of overlapping spreading centers at fast spreading rates (Macdonald et al., 1988a,b) but is characterized by oblique transform offsets of shallow axial valleys rather than curved overlapping axial highs. Phipps-Morgan and Sandwell (1994) have also investigated offset propagation using satellite gravity data and concluded that the migration of offsets on the SEIR is predominantly from west to east. This is true in cases of monotonic propagation but the oscillatory propagating offsets do not show this type of behaviour. Oscillatory propagation appears to have increased in the past 10 Ma but this cannot be demonstrated conclusively with the limited resolution of satellite gravity because some propagat-

Fig. 1. Satellite gravity gradient image of the SEIR (bottom) with earthquakes and isochrons (top). Gradient operator applied from the west to emphasize north–south trending features in the gravity field related to seafloor topography. Satellite gravity data are from Sandwell and Smith (1997) and isochrons are from the gridded age model of Muller et al. (1993). Earthquake epicenters are shown as filled circles and the magnetic anomaly picks constraining the seafloor age model are shown as open circles. Light gray ridge line indicates transitional axial morphology. The planform segmentation is influenced by the presence of the Amsterdam and Kerguelen hotspots near 75°E–80°E and the AAD between 120°E and 125°E. Accentuated fracture zones emphasize the contrast between persistent zero order segment boundaries and more ephemeral first and second order segment boundaries. The boundary between monotonic and oscillatory offset propagation at 100°E is also evident at this scale.

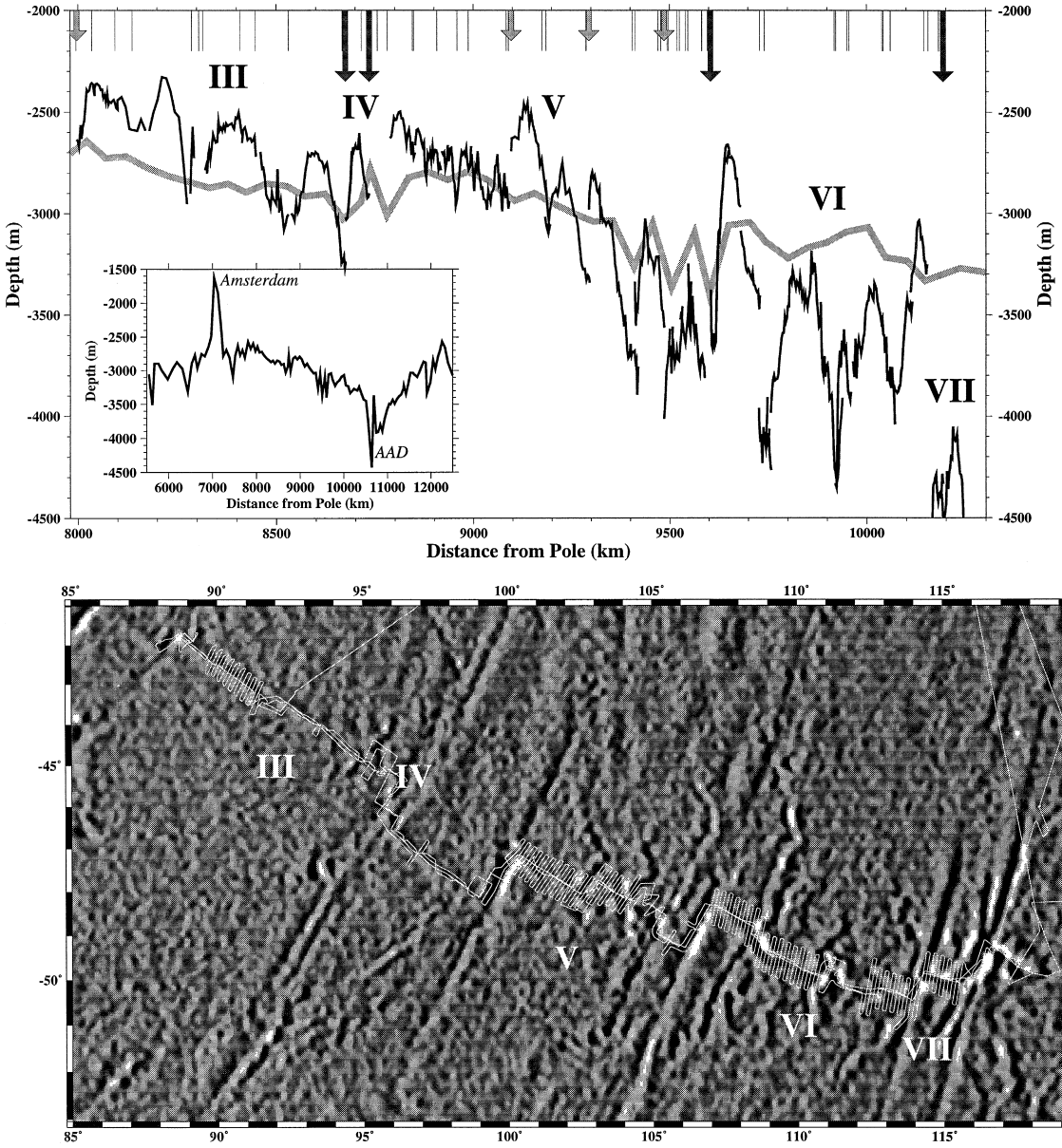

Fig. 2. Band pass filtered satellite gravity gradient image of the SEIR (bottom) and spreading center depths between 88°E and 119°E (top). Black depth profile shows axial depth from multibeam survey and grey profile shows median depth within 50 km of the ridge axis from bathymetry model of Sandwell and Smith (1997). Inset shows regional depth profile for the entire Australian–Antarctic plate boundary. Black arrows indicate zero order segment boundaries, gray arrows indicate transform offsets and thin lines indicate second order offsets. The band pass filter applied to the gravity data has half-power points at 25 and 400 km and gradient operator is applied from the west. Survey tracks of the Westward 9 and 10 expeditions of the R/V *Melville* are shown in white. Roman numerals indicate names of stable zero order segments. Note the transition in offset propagation at 100°E.

ing offsets have low amplitude gravity anomalies. The onset of the most recent episode of oscillatory propagation east of 100°E appears to corrrespond to a 25% increase in spreading rate since 10 Ma

(Fig. 1). This increase in spreading rates may have acted to destabilize the offsets east of 100°E thereby making them more susceptible to migration in the presence of local variations in the stress field near the plate boundary.

4. Present-day segmentation of the SEIR from 88°E to 119°E

The transition at 100°E described above persists in the present-day segmentation and is manifested in both the recent migration of offsets as well as their morphology. West of the transition, non-transform offsets generally take the form of overlapping spreading centers with axial rises while to the east the offsets often appear as non-transform offsets separating axial depressions. Examples of both propagating and stable offsets are shown in Figs. 3 and 4. Analogous types of offsets have been observed extensively on both the Mid-Atlantic Ridge (e.g., Grindlay et al., 1991) and on the East Pacific Rise (e.g., Lonsdale, 1977) and are consistent with the morphologic transition described above. One characteristic of the higher order segmentation that is common throughout the study area is the presence of a pervasively faulted axis with numerous short (<5 km) en-echelon offsets (Fig. 4). The absence of an unfaulted neovolcanic zone over much of the study area is unusual in comparison to most spreading centers. Non-migrating second order offsets in the transitional region often take the form of overlapping fault complexes, similar to conventional overlapping spreading centers (OSCs) but lacking an axial ridge (Fig. 4).

The transition in morphology and segmentation is also manifested by a transition in axial depth. Axial depth, (Fig. 2), is consistently shallower ($\sim$ 2800 m) in segments III and V but increases eastward within the transition of segment V and remains generally deeper ($\sim$ 3700 m) east of segment IV. This deepening of the ridge axis corresponds to a transition from axial high morphology in the west to a morphology dominated by axial depressions and fully developed axial valleys near the AAD. This morphologic transition is discussed in greater detail by Ma and Cochran (1996, 1997) and Shah and Sempéré (1998). Axial relief also increases on the deeper segments east of segment IV as is typical of spreading centers with axial valley morphology (Sempéré et al., 1990). The overall deepening and increasing relief of the axis has been interpreted to be a result of a combination of crustal thinning and colder denser asthenosphere approaching the AAD (Sempéré et al., 1997).

Along axis variations in average flanking depth suggest that the zero order segmentation may continue to play an important role in lithopshere and mantle structure. Flanking depths along the SEIR show a distinctly different pattern from axial depths. Median depths within 50 km of the ridge axis are calculated using the 2′ bathymetry model of Sandwell and Smith (1997). Although this bathymetry model lacks the resolution of the survey data, it is consistent with the centerbeam depths compiled by Ma and Cochran (1997) and shows regional depth variations in areas where off axis multibeam coverage is not available. By averaging within 50 km of the ridge axis, the influence of axial morphology is diminished and the depth variations preserved on older (1–2 Ma) seafloor are emphasized. The inset plot in Fig. 2 indicates that the deepening between Amsterdam and the AAD is more monotonic than is suggested by the axial morphology. A monotonic regional deepening is consistent with the regional gradient in mantle temperature inferred from seismic velocity anomalies (Roult, 1994). Interestingly, two of the three departures from monotonic deepening between Amsterdam and the AAD correspond to the western boundaries of zero order segments V and VI (Fig. 2). The other instance of eastward shallowing in the regional depth occurs near 83°E where asthenospheric flux from the Kerguelen hotspot may be entrained at the plate boundary (Small, 1995).

The pattern of recent seismicity on the ridge axis also highlights the transition in segmentation (Fig. 1). In the region to the west of the transition, teleseismic events are clustered near offsets; in the region to the east of the transition the seismicity also occurs predominantly at offsets but tends to be dispersed over larger regions about the offset with more abundant intra-segment epicenters. The azimuthal coverage of the SEIR is far from optimal for the accurate determination of epicenters and there are likely to be significant location errors in these data but the errors should be distributed evenly over the

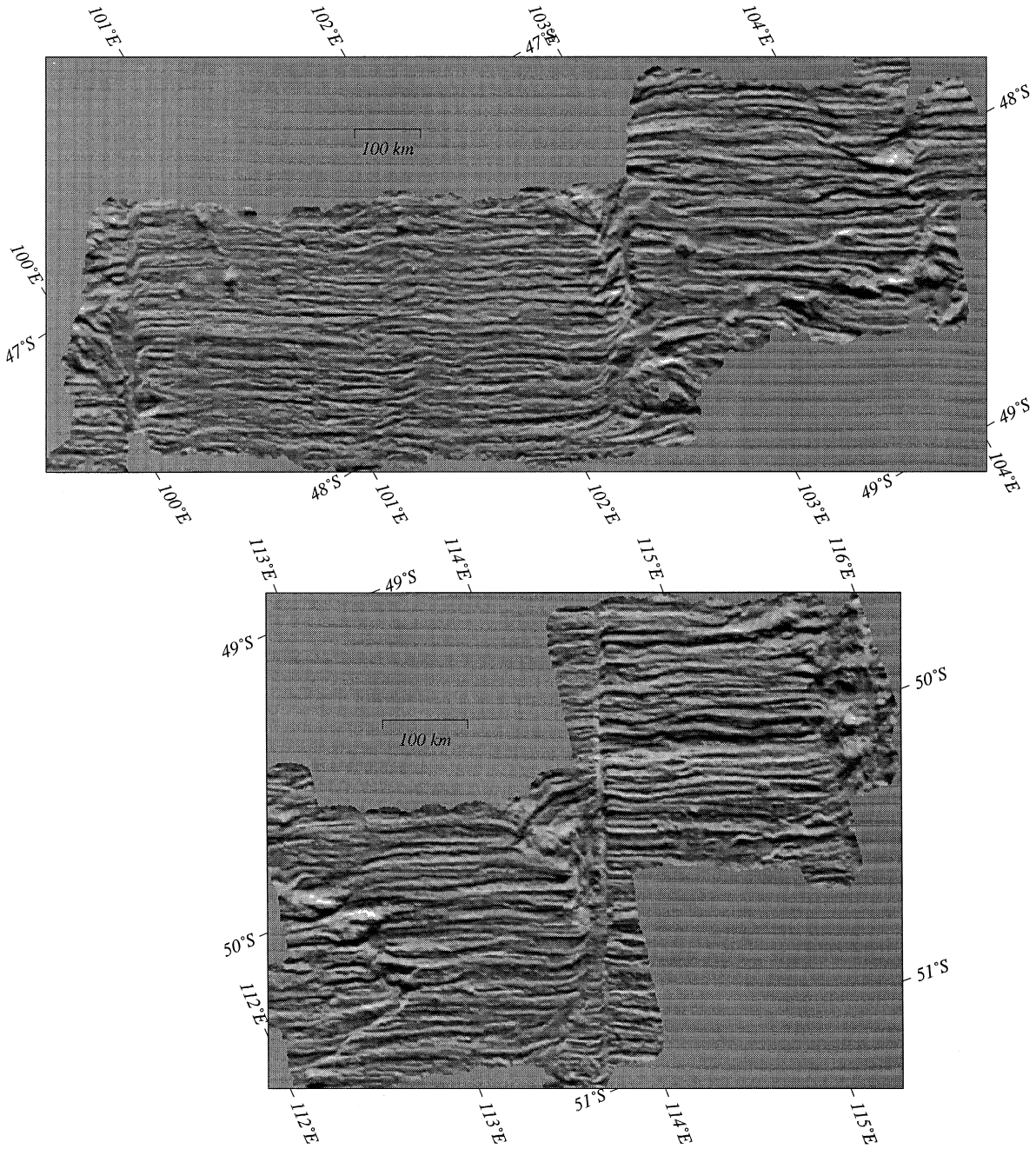

Fig. 3. Example of Seabeam 2000 multibeam bathymetry survey of transitional segments on the SEIR. Gradient operator applied from the south. The upper image shows a gradation from axial rise to transitional morphology. Note the stable second order segment boundary near 101°30′E and the eastward propagating offset near 104°E. The lower image shows a transitional segment abutting an axial valley segment. Note the difference between the two propagating offsets within the transitional segment. The morphology on the western propagator has over 1500 m relief and has propagated at ~50 km/Ma. while that on the eastern propagator has less than 500 m relief and has propagated at ~10 km/Ma. Axial morphology changes from a slight axial depression to a fully developed axial valley across the western transform. The 2000-m depression near 114°E suggests that this transform is transtensional. Both maps plotted in oblique Mercator projection.

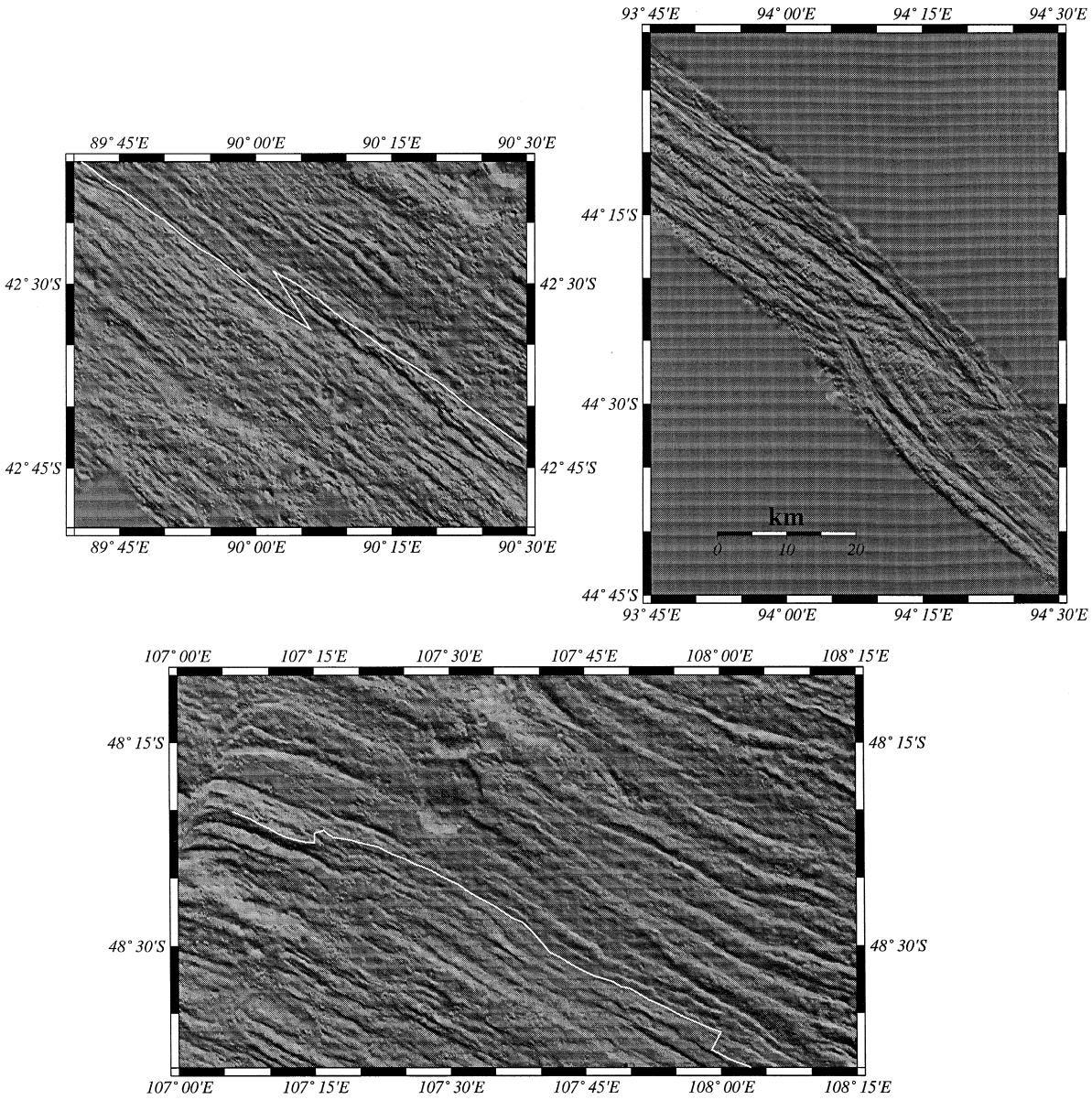

Fig. 4. Example of Seabeam 2000 multibeam bathymetry showing transitional segmentation. Thin white lines show approximate center of the ridge axis. Note the lack of a pronounced axial rise or valley and the diffuse zone of pervasive faulting in each example. Gradient operator applied from the south.

study area. The increase in non-transform seismicity east of the transition corresponds to an increasing number of propagating offsets. While propagating offsets are found throughout the study area, the decrease in crustal thickness east of the transition inferred by Sempéré et al. (1997) would result in an increase in net lithospheric strength which may be manifest by the greater abundance of teleseismic earthquakes. The increased morphologic relief associated with the propagating offsets east of the transition is consistent with a stronger lithosphere capable of accomodating greater stress before experiencing

brittle failure. The implications for segmentation stability are discussed below.

4.1. Recent changes in spreading direction

The present-day transform morphology of the SEIR between 88°E and 118°E shows evidence for a recent counter clockwise change in spreading direction. Currently available ridge flank bathymetry data do not provide sufficient coverage to conclusively verify this assertion but the morphology of transform offsets along the ridge axis and the teleseismicity support this interpretation. A counterclockwise change in spreading direction would render right stepping transforms transpressional and left lateral transforms transtensional. The right stepping (left lateral) transforms in the study area are characterized by anomalously shallow topography on one or both sides of a relatively narrow active displacement zone while the left stepping transforms are characterized by relatively broad anomalously deep areas. At 96°E a 92 km long right lateral offset is marked by a narrow, 5–8 km wide ridge with $\sim$ 2000 m relief. In general, the right stepping offsets have step-like relief on the order of 2000 m and the seismicity in the vicinity of these transforms tends to be distributed along trends oblique to the transform suggesting the transfer of stresses into the adjacent lithosphere on either side of the transform. The right stepping offset near 107°E, however, lacks a typical transform morphology and appears to be evolving to eliminate a short spreading segment between the two larger segments. Interestingly, the double right stepping transform at 105°E does not appear to be teleseismically active although the adjacent topography is anomalously shallow similar to the other right stepping transforms. The left stepping transforms in the study area are characterized in most cases by 5–10 km wide deeps similar to those shown in Fig. 3. In one case, near 106°30′E, a closely spaced pair of left lateral transforms contains a 4900 m deep intra-transform spreading segment from which pillow basalts containing fresh glass were dredged. In most cases, seismicity appears to be more concentrated along the transform zone for the left lateral transforms although the accuracy of the epicentral locations may not be sufficient to base the argument on seismicity alone.

5. Diffuse deformation and metastable segmentation

Along-axis variations in the higher order segmentation of the SEIR correspond to variations in the axial morphology and suggest that the evolution of segmentation is related to transitions in axial morphology. The narrow axial rises found along the East Pacific Rise are remarkably continuous along axis and tend to be offset by well defined OSCs. Axial valleys at slow spreading ridges also generally contain well defined neovolcanic zones with distinct non-transform offsets. In contrast, the transitional morphology of the SEIR generally lacks a narrow well defined neovolcanic zone delineated by unfaulted flows and volcanic edifices. The axis of the SEIR is generally characterized by numerous en-echelon offsets of a broad axial deformation zone delineated by the axis of symmetry of steep inward dipping faults (Fig. 4). This distinctive axial morphology suggests a different relationship between extensional deformation and magmatism than is observed at either fast or slow spreading mid-ocean ridges.

The character of both the morphology and the segmentation can be explained by diffuse deformation at a broad plate boundary zone. At lower spreading rates, the width of the rheologically weak zone where lithospheric deformation occurs is localized by the steep, age dependent isotherms leading to large gradients in lithospheric strength near the axis. At intermediate rates the horizontal gradient in lithospheric strength (with distance) is significantly smaller so the age dependent strengthening does not create as narrow a weak zone (relative to the thickness of the crust and hydrothemally strengthened lithosphere) and deformation can occur over a broader plate boundary zone. At faster spreading rates the mantle temperature becomes sufficiently elevated to allow pervasive melting of the upwelling asthenosphere and segregation of the melt beneath the ridge axis. Once the combination of spreading rate and ambient mantle temperature can maintain a axial magma chamber, the deformation becomes focused on a narrow (< 10 km) weak zone. The persistence of a narrow magma chamber maintains the localized weak zone at the plate boundary and provides a continuous, well defined minimum in lithospheric

strength where extensional deformation is focused. Without this persistent narrow weak zone the deformation of the lithosphere is dictated only by age dependent strengthening and can occur over a wider region. This diffuse deformation zone is more susceptible to spatiotemporal variations in mantle temperature and composition because it lacks the positive feedback between lithospheric weakening and asthenospheric upwelling. Time dependent intrasegment scale variations in lithospheric strength acting on the broad deformation zone may then produce instability in higher order segmentation as a result of interactions between the stress fields associated with strong and weak regions.

6. Conclusions

Both the morphology and the planform segmentation of the central SEIR are influenced by the presence of the Amsterdam and Kerguelen hotspots and the AAD. A gradation in morphology and segmentation exists at a single intermediate spreading rate between these two features as a result of local and regional mantle temperature variations. The large scale segmentation of the plate boundary has been preserved in the form of several zero order segments which have remained stable in the presence of migrating offsets. First order segments are transient and may appear and disappear both by offset propagation and lenthening and shortening of transforms. Transform offsets throughout the survey area show morphology consistent with a recent counterclockwise change in spreading direction.

There exists a transition near 100°E between distinct morphologies, segmentation patterns and spreading center dynamics to the east and west. To the west of the 100°E transform, offset propagation has occurred monotonically eastward and currently takes the form of migrating overlapping axial highs while to the east propagation has occurred in an oscillatory fashion and is marked by rugged topography and offset axial deeps. The pattern of axial depth also changes profoundly within the transitional region; mean axial depth is nearly 1000 m greater east of the transition and mean axial relief increases by a factor of two. In contrast, average flanking depths do not preserve dynamic axial topography and reveal a more gradual deepening approaching the AAD. An increase in the degree of oscillatory propagation to the east of 100°E corresponds to an increase in spreading rates during the past 10 Ma. This increase in spreading rates may have acted to destabilize the offsets east of 100°E thereby making them more susceptible to migration in the presence of local variations in the stress field of the plate.

The transition in axial depth and relief may be explained by differences in lithospheric structure related to the thermal gradient in the study area. Sempéré et al. (1997) have proposed that the crustal thickness is greater in the western part of the study area. The increase in lithospheric strength associated with thinner crust could explain the different styles of offset propagation and seismicity patterns near the AAD. The presence of a broad plate boundary deformation zone on intermediate spreading ridges where focused upwelling and melt production do not maintain a localized weak zone may explain the instability of second order spreading segments.

Acknowledgements

We would like to thank John Sclater and an anonymous reviewer for helpful comments. C.S. and J.R.C. were supported by National Science Foundation grant OCE-9302091 and a Lamont-Doherty Postdoctoral Research Fellowship (to C.S.). D.C. and J.C.S. were supported by National Science Foundation grant OCE-9403583

References

Chen, Y., Morgan, W.J., 1990a. Rift valley/no rift valley transition at mid-ocean ridges. J. Geophys. Res. 95, 17571–17581.

Chen, Y., Morgan, W.J., 1990b. A nonlinear rheology model for mid-ocean ridge topography. J. Geophys. Res. 95, 17583–17604.

Cochran, J.R., 1986. Variations in subsidence rates along intermediate and fast spreading mid-ocean ridges. Geophys. J. R. Astron. Soc. 87, 421–454.

Cochran, J.R., Sempéré, J.C., Christie, D., Eberle, M., Geli, L., Goff, J.A., Kimura, H., Ma, Y., Shah, A., Small, C., Sylvander, B., West, B.P., Zhang, W., 1997. The Southeast Indian Ridge between 88°E and 120°E: gravity anomalies and crustal accretion at intermediate spreading rates. J. Geophys. Res. 102, 15506–15520.

Forsyth, D.W., Ehrenbard, R.L., Chapin, S., 1987. Anomalous

upper mantle beneath the Australian–Antarctic Discordance. Earth Planet. Sci. Lett. 84, 471–478.

Grindlay, N.R., Fox, P.J., Macdonald, K.C., 1991. Second-order ridge axis discontinuities in the south Atlantic: morphology, structure, and evolution. Mar. Geophys. Res. 13, 21–50.

Hayes, D.E., Kane, K.A., 1994. Long-lived mid-ocean ridge segmentation of the Pacific–Antarctic ridge and the Southeast Indian ridge. J. Geophys. Res. 99, 19679–196592.

LePichon, X., Heirtzler, J.R., 1968. Magnetic anomalies in the Indain Ocean and sea-floor spreading. J. Geophys. Res. 73, 2101–2117.

Lonsdale, P., 1977. Structural geomorphology of a fast-spreading rise crest: the East Pacific Rise near 3°25′S. Mar. Geophys. Res. 3, 251–293.

Ma, Y., Cochran, J.R., 1997. Bathymetric roughness of the Southeast Indian Ridge: implications for crustal accretion at intermediate spreadiing rate mid-ocean ridges. J. Geophys. Res. 102, 17697–17711.

Macdonald, K.C., Fox, P.J., Perram, L.J., Eisen, M.F., Haymon, R.M., Miller, S.P., Carbotte, S.M., Cormier, M.H., Shor, A.N., 1988a. A new view of the mid-ocean ridge system from behaviour of ridge-axis discontinuities. Nature 335, 217–225.

Macdonald, K.C., Haymon, R.M., Miller, S.P., Sempéré, J.C., Fox, P.J., 1988b. Deep-tow and sea beam studies of dueling propagating ridges on the East Pacific Rise near 20°40′S. J. Geophys. Res. 93, 2875–2898.

McKenzie, D.P., Sclater, J.G., 1971. The evolution of the Indian Ocean since the late Cretaceous. Geophys. J. R. Astron. Soc. 25, 437–528.

Muller, R.D., Royer, J.Y., Lawver, L.A., 1993. A review of absolute plate motion models from Jurassic to present day. Univ. Texas Inst. Geophys. 112.

Palmer, J., Sempéré, J.-C., Phipps Morgan, J., Christie, D., 1993. Morphology and tectonics of the Australian–Antarctic Discordance. Mar. Geophys. Res. 15, 121–152.

Phipps-Morgan, J., Sandwell, D.T., 1994. Systematics of ridge propagation south of 30°S. Earth Planet. Sci. Lett. 121, 245–258.

Royer, J.Y., Schlich, R., 1988. Southeast Indian Ridge between the Rodriguez Triple Junction and the Amsterdam and Saint-Paul Islands: detailed kinematics for the past 20 m.y. J. Geophys. Res. 93, 13524–13550.

Sandwell, D.T., Smith, W.H.F., 1997. Marine gravity anomaly from Geosat and ERS-1 satellite altimetry. J. Geophys. Res. 102, 10039–10054.

Schlich, R., 1975. Structure et age de l'ocean Indien occidental. Mem. Hors-Ser. Soc. Geol. Fr. 6, 103.

Schlich, R., 1982. The Indian Ocean: aseismic ridges, spreading centers, and oceanic basins. In: Nairn, A.E.M., Stehli, F.G. (Eds.), Ocean Basins and Margins: Vol. 6. The Indian Ocean. Plenum, New York, 1982, pp. 51–147.

Schlich, R., Patriat, P., 1967. Profils magnetiques sur la dorsale medio-oceanique ''Indo-Pacifique''. Ann. Geophys. 23, 629–663.

Sclater, J.G., Fischer, R.L., 1974. Evolution of the east-central Indian Ocean with emphasis on the tectonic setting of the Ninetyeast Ridge. Geol. Soc. Am. Bull. 85, 683–702.

Sempéré, J.C., Purdy, G.M., Schouten, H., 1990. Segmentation of the Mid-Atlantic Ridge between 24°N and 30°40N. Nature 344, 427–431.

Sempéré, J.C., Cochran, J.R., Christie, D., Eberle, M., Geli, L., Goff, J., Kimura, H., Ma, Y., Shah, A., Small, C., Sylvander, B., West, B., Zhang, W., 1997. The Southeast Indian Ridge between 88°E and 118°E: variations in crustal accretion at constant spreading rate. J. Geophys. Res. 102, 14489–15505.

Shah, A., Sempéré, J.-C., 1998. Morphology of the transition from an axial high to an axial valley at the Southeast Indian Ridge and the relation to variations in mantle temperature. J. Geophys. Res. 103, 5203–5223.

Small, C., 1995. Observations of ridge-hotspot interaction in the Southern Ocean. J. Geophys. Res. 100, 17931–17946.

Small, C., Sandwell, D.T., 1989. An abrupt change in ridge axis gravity with spreading rate. J. Geophys. Res. 94, 17383–17392.

Small, C., Sandwell, D.T., 1994. Imaging mid-ocean ridge transitions with satellite gravity. Geology 22, 123–126.

Small, C., Royer, J.Y., Sandwell, D.T., 1989. Discontinuous geoid roughness along the Southeast Indian ridge. EOS 70.

Su, W.J., Woodward, R.L., Dziewonski, A.M., 1994. Degree 12 model of shear velocity heterogeneity in the mantle. J. Geophys. Res. 99, 6945–6980.

Stein, S., Melosh, H.J., Minster, J.B., 1977. Ridge migration and asymmetric sea-floor spreading. Earth Planet. Sci. Lett. 36, 51–62.

Vogt, P.R., Cherkis, N.Z., Morgan, G.A., 1984. Project Investigator: 1. Evolution of the Australia–Antarctic Discordance from a detailed aeromagnetic study. In: Oliver, R.L., James, P.R., Jago, J.B. (Eds.), Antarctic Earth Science. Canberra, 1984.

Weissel, J.K., Hayes, D.E., 1974. The Australian–Antarctic Discordance: new results and implications. J. Geophys. Res. 197, 2579–2587.